Entanglement dynamics of the ultra-strong coupling three-qubit Dicke model

Lijun Mao,[1] Yanxia Liu,[1] and Yunbo Zhang[1,*]

[1]*Institute of Theoretical Physics, Shanxi University, Taiyuan 030006, P. R. China*

We give an analytical description of the dynamics of the three-qubit Dicke model using the adiabatic approximation in the parameter regime where the qubits transition frequencies are far off-resonance with the field frequency and the interaction strengths reach the ultra-strong coupling regimes. Qualitative differences arise when comparing to the single- and two-qubit systems - simple analytic formulas show that three revival sequences produce a three-frequency beat note in the time evolution of the population. We find an explicit way to estimate the dynamics for the qubit-field and qubit-qubit entanglement inside the three-qubit system in the ultra strong coupling regime, and the resistance to the sudden death proves the robustness of the GHZ state.

PACS numbers: 42.50.Pq, 42.50.Md, 03.65.Ud,

arXiv:1512.06387v1 [quant-ph] 20 Dec 2015

I. INTRODUCTION

Recent experimental studies have shown that the ultrastrong coupling regime, where the coupling strength is some tenths of the mode frequency, can be achieved in a number of implementations such as superconducting circuits [1–4], semiconductor quantum wells [5–7], possibly also in surface acoustic waves [8] and trapped ions [9]. The fast-growing interest in the ultrastrong coupling regime is motivated not only by theoretical predictions of novel fundamental properties [10–12] but also by potential applications in quantum computing tasks [13, 14]. The advent of these impressive experimental results prompts a number of theoretical efforts to give analytical solutions for the quantum Rabi and Dicke models [15, 16] by applying various techniques [17–21]. On the other hand, the models are expanded to more general cases, including different qubits [22–26], anisotropic couplings [27–29], a finite-size ensemble of interacting qubits [30] and two-photon interactions [31], to name only a few.

In particular, people start to tackle the entanglement features both between the qubit and the field and inside the qubit system, yet with the rotating wave approximation [32–35]. Entanglement, as a fundamental quantum mechanical tool describing the non-local correlations between quantum objects, lies at the heart of quantum information sciences [36–38]. It is highly expected that nontrivial population and entanglement dynamics would emerge in the ultrastrong coupling regime where the RWA fails. For the Rabi model, a displaced Fock state method [39] is developed to analytically predict the time evolution of the qubits occupation probability in the case of strong coupling and large detuning. The key step is the adiabatic approximation which nicely truncates the system Hamiltonian into a block diagonal form and the resulted solutions are utilized to study the entanglement dynamics in the two-qubit system [25, 40]. Specifically, a simple expression of the concurrence [41] for the two qubits is given analytically and the entanglement sudden death appears even in the inhomogeneous coupling case. The circuit quantum electrodynamics (QED) architecture offers considerable potential for simulating such dynamics following an analog-digital approach [42].

The motivation of this study is stimulated by a lack of an analytical analysis of the bipartite entanglement inside the multi-qubit system in the ultras-trong coupling regime. Typical model for this is the three-qubit Dicke model characterized by a realistic realization of a GHZ state [43]. Recently, it has been shown that superconducting circuit technology allows to exploit the the dynamical Casimir effect physics as a useful resource for the generation of highly entangled states for multi superconducting qubits [44]. It is thus desirable to demonstrate whether the sudden death of entanglement would survive the dissipative effects for the strong and ultrastrong coupling regimes [45]. Here, we show the robustness of three-qubit GHZ state against the interaction and the energy exchange between the qubits and the field in the Dicke model, which could be of importance for future applications e.g. in quantum cryptography [46, 47], quantum computation [48] and quantum gates [49–51].

This paper is organized as follows. We solve the three-qubit Dicke model in a spin-3/2 subspace and derive the analytical eigen solutions by means of the adiabatic approximation in Sec. II. These results are applied to study the population dynamics of the three qubits coupled to, respectively, a Fock state and a coherent state of the oscillator in Sec. III. The spectrum of the multi-revival signal is analyzed and compared to the numerical calculation without the adiabatic approximation. Then, we explore the entanglement dynamics for three qubits starting from the GHZ state and the field in a coherent state and show the robustness of the GHZ state through the bipartite entanglement measure I tangle in Sec. V. Finally, a brief summary is presented in Sec. VI.

*Electronic address: ybzhang@sxu.edu.cn

II. EIGENSOLUTION OF THE THREE-QUBIT DICKE MODEL

We consider the three-qubit Dicke model described by the following Hamiltonian ($\hbar = 1$) [16, 19, 20]

$$H = \omega_c a^\dagger a - \omega J_x + 2g\left(a^\dagger + a\right) J_z. \tag{1}$$

Here $a^\dagger$ (a) is the creation (annihilation) operator of the single bosonic mode with frequency ω_c, ω denotes the qubit splitting, the constant g represents the coupling between the qubit and field mode, and the total spin operator is the sum of the Pauli operators of the individual qubits, i.e. $J_i = \sum_{\alpha=1}^{3} \sigma_i^\alpha/2$ ($i = x, y, z$). Note that J^2 commutes with the Hamiltonian (1), i.e. $\left[J^2, H\right] = 0$, this provides a splitting of the eight-dimensional spin space into a quadruplet state space $j = 3/2$ and two doublet state spaces $j = 1/2$,

$$H = H^{3/2} \oplus H^{1/2} \oplus H^{1/2}. \tag{2}$$

which comes from three possible standard Young tableaux $\boxed{1}\boxed{2}\boxed{3}$, $\begin{array}{|c|c|}\hline 1 & 2 \\ \hline 3 \\ \cline{1-1}\end{array}$, and $\begin{array}{|c|c|}\hline 1 & 3 \\ \hline 2 \\ \cline{1-1}\end{array}$ in representation theory of permutation group theory [52]. The three-qubit Dicke model thus decomposes into a system of one spin-3/2 and two spin-1/2 Rabi models [19]. While both models have been solved using the displaced Fock space method [17, 20, 39] and Bargmann-space techniques [18, 19], little attention has been paid to the analytical dynamics of the qubit occupation probability due to the cumbersome task in extracting the analytical solution in both formulations. Indeed the power series must be terminated in the transcendental function $G_\pm(x)$ [18], or the expansion of the wave function in terms of displaced Fock space should be truncated in a finite N_{tr} subspace [17, 20].

Here, similar to the cases of single- [17, 39] and two-qubit [25, 40] Rabi model, we apply the adiabatic approximation to the numerical solutions when the frequencies of the qubits are much smaller than the oscillator frequency $\omega \ll \omega_c$. In this displaced oscillator basis the Hamiltonian may be truncated to a block-diagonal form and the blocks solved individually. We shall confine ourselves in the following to the system with four-dimensional spin-subspace of $j = 3/2$, due to the fact that all interesting dynamics in the three-qubit system prepared in the experiments is confined in this subspace, and best of all, this method is the most effective way to study analytically the dynamical properties of three qubits. The Hamiltonian $H^{3/2}$ reduces to 4×4 block diagonal form, i.e. $H^{3/2} = \sum_{n=0}^{\infty} \oplus H_n$ with

$$H_n = \begin{pmatrix} \epsilon_{3/2}^n & \sqrt{3}\Omega_n & 0 & 0 \\ \sqrt{3}\Omega_n & \epsilon_{1/2}^n & 2\Omega_n & 0 \\ 0 & 2\Omega_n & \epsilon_{1/2}^n & \sqrt{3}\Omega_n \\ 0 & 0 & \sqrt{3}\Omega_n & \epsilon_{3/2}^n \end{pmatrix}. \tag{3}$$

where $\epsilon_m^n = \omega_c\left(n - \beta_m^2\right)$. The system is spanned by the the joint spin-field space $|3/2, m\rangle\,|n\rangle_{A_m}$ where $|j, m\rangle$ are eigenstates of J^2 and J_z with eigenvalues $j(j+1)$ and $m = -j, -j+1, ..., j$, respectively, and the displaced Fock states satisfy $A_m^\dagger A_m\,|n\rangle_{A_m} = n\,|n\rangle_{A_m}$ with $A_m = a + \beta_m$ and $\beta_m = m\alpha$ and $\alpha = 2g/\omega_c$. The off-diagonal elements in the matrix are given by

$$\Omega_n = -\frac{\omega}{2} e^{-\frac{\alpha^2}{2}} \sum_{l=0}^{n} \frac{(-1)^{n-l} n!}{l![(n-l)!]^2} \alpha^{2(n-l)}. \tag{4}$$

It can be easily proved that the parity operator defined in the spin-3/2 subspace as $\Pi^{3/2} = \exp\left[i\pi\left(3/2 - J_x + a^\dagger a\right)\right]$ with eigenvalues $\kappa = \pm 1$, commutes with the Hamiltonian, i.e. $\left[H^{3/2}, \Pi^{3/2}\right] = 0$. Accordingly, the Hilbert space splits into two mutually orthogonal subspaces with even and odd parities [19]. The four eigenstates of H_n are non-degenerate and can be classified uniquely by one quantum number. However, for numerical solutions beyond the adiabatic approximation, it is necessary to use the parity operator to classify the degeneracies that take place between levels of states with different parity. For consistency, we use parity invariance $[H_n, \Pi_n] = 0$ with Π_n an anti-diagonal matrix $(-1)^n \mathrm{adiag}[1, 1, 1, 1]$, to further block diagonalize H_n as $H_n = \sum_{\kappa=\pm1} \oplus H_n^\kappa$ with

$$H_n^\kappa = \begin{pmatrix} \epsilon_{3/2}^n & \sqrt{3}\Omega_n \\ \sqrt{3}\Omega_n & \epsilon_{1/2}^n + 2\xi\Omega_n \end{pmatrix} \tag{5}$$

and $\xi = \kappa\,(-1)^n$. The energy levels are given by

$$E_n^{\kappa\pm} = n\omega_c + \xi\Omega_n - 5g^2/\omega_c \pm \theta_n^\kappa \tag{6}$$

with $\theta_n^\kappa = \sqrt{(\xi\Omega_n + 4g^2/\omega_c)^2 + 3\Omega_n^2}$. The corresponding eigenstates in the spin-field space are

$$\left|\psi_n^{\kappa\pm}\right\rangle = d_n^{\kappa\pm}\left(c_n^{\kappa\pm}, 1, \xi, \xi c_n^{\kappa\pm}\right)^T \tag{7}$$

with $c_n^{\kappa\pm} = \sqrt{3}\Omega_n/\left(\xi\Omega_n + 4g^2/\omega_c \pm \theta_n^\kappa\right)$ and $d_n^{\kappa\pm} = 1/\sqrt{2\left|c_n^{\kappa\pm}\right|^2 + 2}$. We restrict the analysis in the following to the case of $|\Omega_n| \gg 4g^2/\omega_c$ fulfilled by most experimental systems in the ultra-strong coupling regime $g \leq 0.08\omega_c$, which enables us to achieve an analytical dynamics below. The eigenvalues are therefore simplified to

$$E_n^{\kappa\pm} = n\omega_c + (\xi \mp 2)\Omega_n, \tag{8}$$

and the corresponding eigenfunctions are

$$\left|\psi_n^{\kappa\pm}\right\rangle = \sqrt{\frac{2 \mp \xi}{8}}\left(\frac{\sqrt{3}}{\xi \mp 2}, 1, \xi, \frac{\xi\sqrt{3}}{\xi \mp 2}\right)^T. \tag{9}$$

We observe that the parity κ and the photon number n in the displaced Fock state are independent to each other. This is due to the fact that in constructing the unitary transformation which brings the Hamiltonian into a block diagonal form (5), a phase difference $n\pi$ is introduced in

the superposition of two displaced Fock states $|n\rangle_{A_m}$ in opposite directions so that symmetric and antisymmetry superposition states of the corresponding bases are respectively even and odd parities. This situation resembles the parity of the ground state and the first excited state in the standard quantum tunneling model of double well potential.

III. POPULATION DYNAMICS

After a detailed discussion of the energy spectrum, we now turn to the study of population dynamics of the qubits. In particular, we will examine the dynamics with all three qubits being excited to the upper level $|eee\rangle$, while the initial state of the oscillator is prepared in the displaced Fock basis corresponding to it, i.e. $|\Psi(0)\rangle = |3/2,3/2\rangle\,|n\rangle_{A_{3/2}}$, which is expressed as the linear combination of the eigenvectors (7)

$$|\Psi(0)\rangle = \sum_{\kappa,\tau} d_n^{\kappa\tau} c_n^{\kappa\tau}\,|\psi_n^{\kappa\tau}\rangle\,. \tag{10}$$

Then at subsequent time t the probability to find three qubits in the initial state $|3/2,3/2\rangle$ is easily obtained

$$P_1(n,t) = \left|{}_{A_{3/2}}\langle n|\,\langle 3/2,3/2|\Psi(t)\rangle\right|^2. \tag{11}$$

Substituting the simplified eigensolutions (8) and (9) into Eq. (11), we find that the probability is composed of three oscillating frequencies

$$\begin{aligned} P_1(n,t) &= \frac{1}{32}\left(10+15\cos(2\Omega_n t)\right. \\ &\quad \left.+6\cos(4\Omega_n t)+\cos(6\Omega_n t)\right), \end{aligned} \tag{12}$$

while in the single- and two-qubit Rabi models we have respectively one and two frequencies dominating the evolution.

If instead, initially the oscillator is displaced from a coherent state $|z\rangle$, i.e.

$$|\Psi(0)\rangle = \sum_{n=0}^{+\infty} \frac{e^{-|z|^2/2} z^n}{\sqrt{n!}}\,|3/2,3/2\rangle\,|n\rangle_{A_{3/2}}\,, \tag{13}$$

which is the closest quantum state to a classical wave and more realistic for describing the oscillator, the probability of three qubits remaining in their initial state $|3/2,3/2\rangle$ is calculated by tracing over all Fock states as

$$\begin{aligned} P_1(z,t) &= \langle 3/2,3/2|Tr_F\rho(z,t)|3/2,3/2\rangle \\ &= \sum_{n=0}^{+\infty} p(n)\,P_1(n,t)\,. \end{aligned} \tag{14}$$

Here $\rho(z,t) = |\Psi(t)\rangle\langle\Psi(t)|$ is the density matrix of the system and the normalized Poisson distribution is defined as $p(n) = e^{-|z|^2}\,|z|^{2n}/n!$. Following the procedure

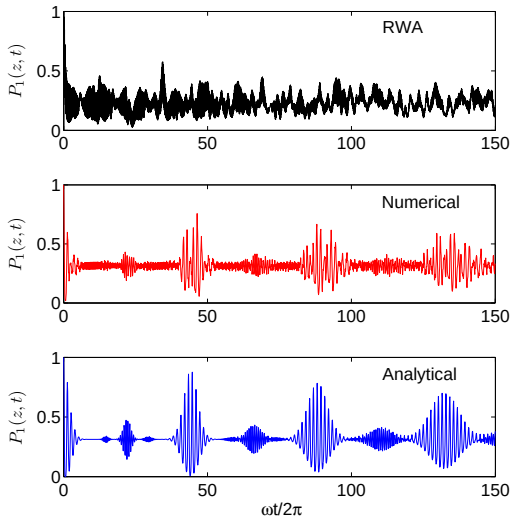

FIG. 1: (Color Online) Probability $P_1(z,t)$ of finding three qubits in the initial state $|3/2,3/2\rangle$ as a function of $\omega t/2\pi$ for $\omega = 0.15\omega_c$, $g = 0.08\omega_c$ and $z = 3$. Note the breakup in the main revival peaks of the numerical evaluation, which comes from the $\omega - 2\omega - 3\omega$ beat note, is not included in the analytic calculation.

established previously for two-qubit model [40] by keeping only three terms $l = n, n-1, n-2$ in the summation of Ω_n and replacing the Poisson distribution by a Gaussian one for big enough $|z|$, we may reduce Eq. (14) into the following analytical form

$$P_1(z,t) = \frac{1}{32}\mathrm{Re}\left[10+15S(t,\omega)+6S(t,2\omega)+S(t,3\omega)\right], \tag{15}$$

with $S(t,\omega) = \sum_{k=0}^{+\infty} S_k(t,\omega)$. The collapse and revival of the probability $P_1(z,t)$, which is approximated with fairly good accuracy by the sufficiently simple function $S_k(t,\omega)$, is obvious here and the individual revival function

$$S_k(t,\omega) = h_k \exp\left(\Phi_{Re} + i\Phi_{Im}\right) \tag{16}$$

with a height $h_k = \left(1+\pi^2k^2f^2\right)^{-1/4}$ and

$$\Phi_{Re} = -\frac{1}{2}h_k^4\left(\mu-\mu_k\right)^2 f\alpha^2, \tag{17}$$

$$\Phi_{Im} = \frac{1}{2}\tan^{-1}(\pi k f) + \mu(1-f) + 2\pi k|z|^2, \tag{18}$$

describes the evolution around the k-th revival time $t_k^{rev} = \mu_k/\omega$ where we have defined $f = |\alpha z|^2$, $\mu = \omega t e^{-\alpha^2/2}$, and $\mu_k = \pi k\left(f+2\right)/\alpha^2$. During each peroid $\Delta t = \pi\left(f+2\right)/\omega\alpha^2$, however, the signals in $S_k(t,2\omega)$ and $S_k(t,3\omega)$ revive twice and three times respectively. We thus get three revival sequences in the evolution of the probability $P_1(z,t)$. The envelope and the fast oscillatory of the revival signal are determined by Φ_{Re} and Φ_{Im} respectively [40].

In Fig. 1, a comparison of the analytic formula derived for $P_1(z,t)$ and the numerical calculations is made in the parameter regime where the coupling strength is strong enough to invalidate the RWA. We see that with the time increasing the equilibrium value 10/32, about which the revival signal oscillates, is smaller than 16/32 in the single qubit model and 12/32 in the two-qubit model [40] due to the involvement of higher order harmonic signals in the probability. The width of the successive revival signals keeps increasing as $\delta\mu_k = \sqrt{1+\pi^2k^2f^2}/|z|\alpha^2$ that leads to the mergence of the third harmonic signal into the first and second ones after several revival periods. The salient feature of the three-qubit model as demonstrated above is that the revival signals corresponding to the three oscillating terms $S(t,\omega), S(t,2\omega)$ and $S(t,3\omega)$ produce a beat note of $\omega - 2\omega - 3\omega$. The three revival sequences in the evolution of $P_1(z,t)$ are even clearer in the Fourier analysis $\bar{P}_1(z,\nu)$ defined as

$$\bar{P}_1(z,\nu) = \int_0^{+\infty} dt P(z,t) e^{-i2\pi\nu t} \tag{19}$$

which is presented in Fig. 2. The spectral signals $\bar{P}_1(n,\nu)$ corresponding to the probability of displaced Fock state are δ functions located at $2\Omega_n$, $4\Omega_n$ and $6\Omega_n$, respectively. The involvement of Fock states of many photons in the coherent state leads to a broad distribution of the spectral functions for $P_1(z,t)$ at a fundamental frequency $\omega^* = \omega e^{-\alpha^2/2}(1-|z|^2\alpha^2)$, which is 0.76ω for $g = 0.08\omega_c$ and $z = 3$, as well as at the second and third harmonics with decreasing magnitude. This contrasts the single and double revival sequences for the single and two-qubit systems as a consequence of having only one and two Rabi frequencies, respectively, which have been showed in [40]. The analytical results reproduce the multiple revival sequences for the three-qubit model, except that breakups appear in the main and the second harmonic revival frequencies if no adiabatic approximation is made, which can be compared with the RWA case in [53]. We find that the RWA completely breaks down in the ultra strong coupling parameter regime considered here.

IV. ENTANGLEMENT BEHAVIORS

The entanglement properties of two identical qubits strongly coupled to a single-mode radiation field have recently been studied in [40, 54], where the entanglement sudden death does appear in the numerical and analytic calculations. However, qualitative differences should arise in the case of the three-qubit system. It is widely accepted nowadays that entangled states of multi-particle systems are the most promising resource for quantum information processing [55–57]. Thus, it is highly desirable to explore the entanglement dynamics of the three-qubit Dicke model.

In this section we provide an easily computable formula for the entanglement dynamics when the field is initially

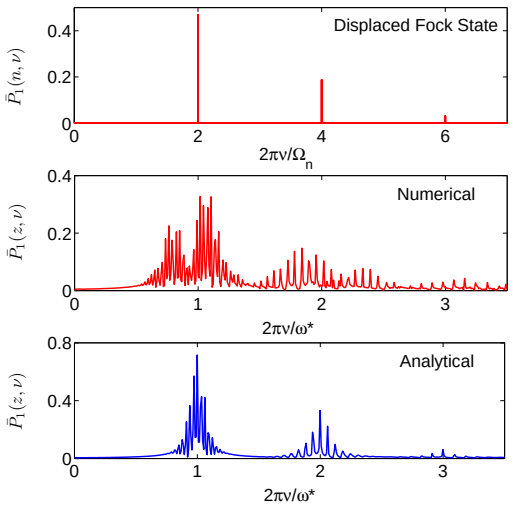

FIG. 2: (Color Online) The Fourier analysis of the probability revival for the displaced Fock state (top) and displaced coherent state (middle and bottom panels for numerical and analytical calculation respectively) of the oscillator with all three qubits being excited to the upper level. Three revival sequences in the dynamics produce a beat note of $\omega - 2\omega - 3\omega$ and the breakups in the fundamental and the second harmonic frequencies without the adiabatic approximation. The corresponding parameters are the same as in Figure 1.

in a coherent state $|z\rangle$ and the three qubits are initially in the form of a familiar GHZ state $\frac{1}{\sqrt{2}}(|eee\rangle + |ggg\rangle)$, i.e.

$$|\Psi(0)\rangle = \frac{1}{\sqrt{2}}(|3/2,3/2\rangle + |3/2,-3/2\rangle)|z\rangle. \tag{20}$$

For small values of α, we may expand the state $|n\rangle$ in the displaced Fock space and the most important contribution in the summation over n comes from the terms with the same n, which is equivalent to take $|n\rangle \approx |n\rangle_{A_m}$ [40]. This approximation gives the state at subsequent time t as

$$|\Psi(t)\rangle = \sum_{n,\kappa\tau} \sqrt{\frac{p(n)}{2}}(1+\xi) d_n^{\kappa\tau} c_n^{\kappa\tau} |\psi_n^{\kappa\tau}\rangle e^{-iE_n^{\kappa\tau}t}. \tag{21}$$

To examine the entanglement evolution of the system we calculate the reduced density matrix of the qubits by tracing over the quantum field

$$\rho_Q(t) = \sum_n \langle n|\Psi(t)\rangle \langle \Psi(t)|n\rangle, \tag{22}$$

which can be reduced to the following matrix form

$$\rho_Q(t) = \begin{pmatrix} \frac{1}{4} & 0 & \frac{\sqrt{3}S(t,2\omega)}{4} & 0 \\ 0 & 0 & 0 & 0 \\ \frac{\sqrt{3}S^*(t,2\omega)}{4} & 0 & \frac{3}{4} & 0 \\ 0 & 0 & 0 & 0 \end{pmatrix} \tag{23}$$

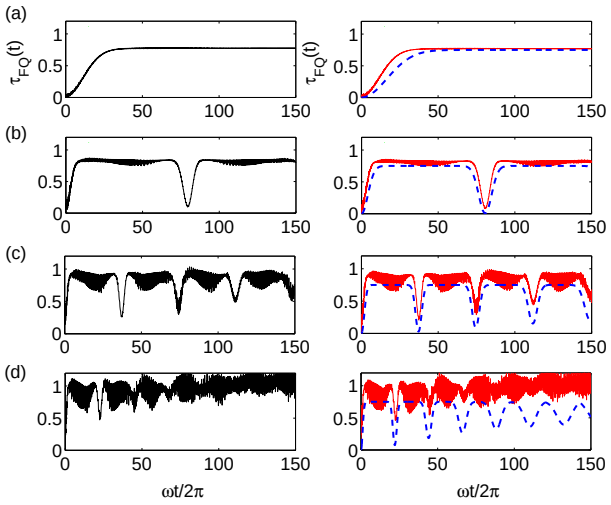

FIG. 3: (Color Online) The I tangle between the qubits and light field as a function of $\omega t/2\pi$ for transition frequency $\omega = 0.15\omega_c$ and different coupling strengthes $g = 0.02\omega_c(a), 0.04\omega_c(b), 0.06\omega_c(c)$ and $0.08\omega_c(d)$, given by numerical method (left), the adiabatic approximation (red solid line, right) and analytical approach (blue dashed line, right).

in the eigen basis $|3/2, m\rangle_x$ of spin J_x.

The entanglement between the field and the qubits may be described by the I tangle

$$\tau_{FQ}(t) = 2\left(1 - tr\left(\rho_Q^2\right)\right), \tag{24}$$

which is introduced in [58] and applicable to infinite-dimensional bipartite systems [34]. It runs from zero for a product state to the maximum value $2(d-1)/d = 1.75$ with $d = \min(d_1, d_2)$ for a maximally entangled state, where d_1, d_2 are respectively the dimensions of the three-qubit system and the photon field. The analytic expression for the reduced density matrix (23) allows us to obtain the explicit formula

$$\tau_{FQ}(t) = \frac{3 - 3|S(t, 2\omega)|^2}{4}. \tag{25}$$

In Fig. 3 we plot the time evolution of I tangle τ_{FQ} for various values of g. Should we adopt the expression (7) for the eigenstates $|\psi_n^{\kappa\tau}\rangle$ and do not take into account $|n\rangle \approx |n\rangle_{A_m}$, the adiabatic approximation produces a quite accurate result in the ultrastrong coupling regime as shown in the right column of Fig. 3. The analytic result determined by formula (25) agrees well with the envelope of the numerically evaluated result, but fails in describing the long time behavior when the coupling strengths are sufficiently large which is evident in Fig. 3. The I tangle τ_{FQ} starts from zero for the initial product state (20), and undergoes periodic weakening and recovery with the oscillation period getting smaller and smaller for increasing coupling strengths, which however could never reach the maximum entanglement value of the system. We see that the field-qubit entanglement exhibits collapse and revival and the analytic formula predicts correctly the main features of the individual entanglement revival signals.

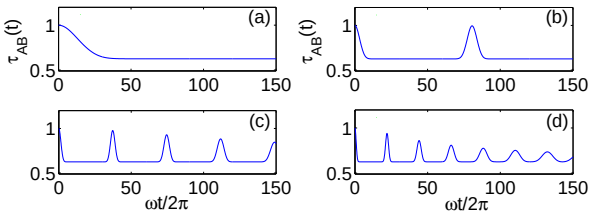

FIG. 4: (Color Online) The I tangle between the three qubits as a function of $\omega t/2\pi$ given by the analytical calcultion. The corresponding parameters are the same as in Figure 3.

The initially pure state of the qubits evolves into a mixed state described by the reduced density matrix ρ_Q in Eq. (23). We may analytically study the entanglement between the qubits in the following. The measures of entanglement for mixed states depend on the pure state decompositions, in this way the main difficulty is to find the minimization over all decompositions of mixed state into pure states. However, our analytic method provides a particular case, where ρ_Q is a rank-2 mixed state of a qubit and a qudit in the basis of the three-qubit product states. Thus we may discuss the properties of the entanglement of three qubits system using the I tangle proposed by Osborne et al. [59]. As a good mixed-state entanglement measure for three qubits, the I tangle $\tau_{AB}(t)$ between one qubit (subsystem A) and the other two qubits (subsystem B) is given by the formula [59]

$$\tau_{AB}(t) = Tr\left(\rho_Q \tilde{\rho}_Q\right) + 2\lambda_{\min}\left[1 - Tr\left(\rho_Q^2\right)\right], \tag{26}$$

where the universal state inverter is defined as $\tilde{\rho}_Q = I_A \otimes I_B - \rho_A \otimes I_B - I \otimes \rho_B + \rho_Q$ with $\rho_A = Tr_B(\rho_Q)$ and $\rho_B = Tr_A(\rho_Q)$ and $\lambda_{\min}$ is the smallest eigenvalue of a real symmetric 3×3 matrix M as defined in [59, 60]. A tedious yet straightforward calculation gives

$$M = \frac{1}{3(1+3|S|^2)} \begin{pmatrix} 2+2|S|^2 & 0 & \frac{4|S|}{\sqrt{3}} \\ 0 & \frac{-1-|S|^2}{2} & 0 \\ \frac{4|S|}{\sqrt{3}} & 0 & \frac{-1+9|S|^2}{3} \end{pmatrix} \tag{27}$$

and $\lambda_{min} = -(1+|S|^2)/(6+18|S|^2)$. Inserting this and the analytic expression (23) into Eq. (26) gives a very simple result for the bipartite entanglement

$$\tau_{AB}(t) = \frac{5 + 20|S(t, 2\omega)|^2 + 7|S(t, 2\omega)|^4}{8\left(1 + 3|S(t, 2\omega)|^2\right)}. \tag{28}$$

The evolution of the I tangle for three qubits is plotted in Fig. 4. In contrast to the field–qubit entanglement $\tau_{FQ}(t)$, it starts from the maximum value and then decreases to a finite steady value where entanglement sudden death is absent. When the field–qubit entanglement

becomes rather weak this qubit-qubit entanglement increases rapidly to a large value, as can be seen in Fig. 3 and Fig. 4. It turns out that the decrease of $\tau_{FQ}(t)$ is directly related to the growth of $\tau_{AB}(t)$ in the form of Eq. (25) and Eq. (28), which predict correctly the time, height, and width of the individual entanglement oscillation. This indicates that the initial entanglement between the qubits withstands the interaction and the energy exchange between the qubits and the field. In this way we provide for the first time an explicit analytical formula for the robustness of the GHZ state in the three-qubit Dicke model.

V. CONCLUSION

In conclusion, we have analyzed the population and entanglement dynamics of three qubits within the adiabatic approximation. It works very well in the ultrastrong coupling regime under the assumption that the qubit frequencies are much smaller than the field frequency. The remarkable feature of population dynamics in the three-qubit model is that the three revival sequences in the evolution of the probability produce a three-frequency beat note. Moreover, the analytic formulas of the I tangle for the pure state of field-qubit system and mixed state of three-qubit exhibit their excellence in entanglement characterization and distribution. This is the first to present the robustness of the GHZ state in the form of the analytic expressions in the three-qubit Dicke model. The sudden death of the entanglement is avoided in the three-qubit system, which are qualitatively different from the two-qubit case studied in [25, 40, 54]. A practically relevant application of our result lies in the quantum information process with circuit QED, where three-qubit entangled states are involved.

Acknowledgements

This work is supported by NSF of China under Grant Nos. 11234008 and 11474189, the National Basic Research Program of China (973 Program) under Grant No. 2011CB921601, Program for Changjiang Scholars and Innovative Research Team in University (PCSIRT)(No. IRT13076).

[1] J. Bourassa, J. M. Gambetta, A. A. Abdumalikov, Jr, O. Astafiev, Y. Nakamura, and A. Blais, Phys. Rev. A **80**, 032109 (2009).
[2] T. Niemczyk, F. Deppe, H. Huebl, E. P. Menzel, F. Hocke, M. J. Schwarz, J. J. Garcia-Ripoll, D. Zueco, T. Hümmer, E. Solano, A. Marx, and R. Gross, Nat. Phys. **6**, 772 (2010).
[3] A. Fedorov, A. K. Feofanov, P. Macha, P. Forn-Díaz, C. J. P. M. Harmans, and J. E. Mooij, Phys. Rev. Lett. **105**, 060503 (2010).
[4] P. Forn-Díaz, J. Lisenfeld, D. Marcos, J. J. García-Ripoll, E. Solano, C. J. P. M. Harmans, and J. E. Mooij, Phys. Rev. Lett. **105**, 237001 (2010).
[5] A. A. Anappara, S. De Liberato, A. Tredicucci, C. Ciuti, G. Biasiol, L. Sorba, and F. Beltram,Phys. Rev. B **79**, 201303(R) (2009).
[6] G. Günter, A. A. Anappara, J. Hees, A. Sell, G. Biasiol, L. Sorba, S. D. Liberato, C. Ciuti, A. Tredicucci, A. Leitenstorfer, and R. Huber, Nature **458**, 178 (2009).
[7] Y. Todorov, A. M. Andrews, R. Colombelli, S. De Liberato, C. Ciuti, P. Klang, G. Strasser, and C. Sirtori, Phys. Rev. Lett. **105**, 196402 (2010).
[8] M. V. Gustafsson, T. Aref, A. F. Kockum, M. K. Ekström, G. Johansson, and P. Delsing, Science **346**, 207 (2014).
[9] J. S. Pedernales, I. Lizuain, S. Felicetti, G. Romero, L. Lamata, and E. Solano, Sci. Rep. **5**, 15472 (2015).
[10] S. Felicetti, T. Douce, G. Romero, P. Milman, and E. Solano, Sci. Rep. **5**, 11818 (2015).
[11] S. De Liberato, Phys. Rev. Lett. **112**, 016401 (2014).
[12] S. Felicetti, G. Romero, D. Rossini, R. Fazio, and E. Solano, Phys. Rev. A **89**, 013853 (2014).
[13] P. Nataf and C. Ciuti, Phys. Rev. Lett. **107**, 190402 (2011).
[14] T. H. Kyaw, S. Felicetti, G. Romero, E. Solano, and L. C. Kwek, Sci. Rep. **5**, 8621 (2015).
[15] I. I. Rabi, Phys. Rev. **49**, 324; *ibid.* **51**, 652 (1936).
[16] R. H. Dicke, Phys. Rev. **93**, 99 (1954).
[17] T. Liu, K. L. Wang, and M. Feng, Europhys. Lett. **86**, 54003 (2009).
[18] D. Braak, Phys. Rev. Lett. **107**, 100401 (2011).
[19] D. Braak, J. Phys. B: At. Mol. Opt. Phys. **46**, 224007 (2013).
[20] Q. H. Chen, Y. Y. Zhang, T. Liu, and K. L. Wang, Phys. Rev. A **78**, 051801 (2008).
[21] S. He, L. W. Duan, and Q. H. Chen, New J. Phys. **17**, 043033 (2015).
[22] J. Peng, Z. Ren, G. Guo, and G. Ju, J. Phys. A: Math. Theor. **45**, 365302 (2012).
[23] J. Peng, Z. Ren, D. Braak, G. Guo, G. Ju, X. Zhang, and X. Guo, J. Phys. A: Math. Theor. **47**, 265303 (2014).
[24] S. A. Chilingaryan, and B. M. Rodríguez-Lara, J. Phys. A: Math. Theor. **46**, 335301 (2013).
[25] L. Mao, S. Huai, and Y. Zhang, J. Phys. A: Math. Theor. **48**, 345302 (2015).
[26] Q. H. Chen, L. W. Duan, and S. He, Ann. Phys. **355**, 121 (2015).
[27] Q. T. Xie, S. Cui, J. P. Cao, L. Amico, and H. Fan, Phys. Rev. X **4**, 021046 (2014).
[28] S. Cui, J. P. Cao, L. Amico, and H. Fan, arXiv:1504.04701 (2015).
[29] H. Zhong, Q. Xie, X. Guan, M. T. Batchelor, K. Gao, and C. Lee, J. Phys. A **47**, 045301 (2014).
[30] R. A. Robles Robles, S. A. Chilingaryan, B. M. Rodríguez-Lara, and R. K. Lee, Phys. Rev. A **91** 033819 (2015).
[31] S. Felicetti, J. S. Pedernales, I. L. Egusquiza, G. Romero, L. Lamata, D. Braak, and E. Solano, Phys. Rev. A **92**,

033817 (2015).
[32] A. S. F. Obada, S. Abdel-Khalek, K. Berrada, and M. E. Shaheen, Physica A **392**, 6624 (2013).
[33] T. E. Tessier, I. H. Deutsch, A. Delgado, and I. Fuentes-Guridi, Phys. Rev. A **68**, 062316 (2003).
[34] M. Youssef, N. Metwally, and A. S. F. Obada, J. Phys. B: At. Mol. Opt. Phys. **43**, 095501 (2010).
[35] C. E. López, G. Romero, F. Lastra, E. Solano, and J. C. Retamal, Phys. Rev. Lett. **101**, 080503 (2008).
[36] J. Preskill, J. Mod. Opt. **47**, 127 (2000).
[37] R. Islam, R. Ma, P. M. Preiss, M. E. Tai, A. Lukin, M. Rispoli, and M. Greiner, Nature **528**, 77 (2015).
[38] B. Hensen, H. Bernien, A. E. Dréau, A. Reiserer, N. Kalb, M. S. Blok, J. Ruitenberg, R. F. L. Vermeulen, R. N. Schouten, C. Abellán, W. Amaya, V. Pruneri, M. W. Mitchell, M. Markham, D. J. Twitchen, D. Elkouss, S. Wehner, T. H. Taminiau, and R. Hanson, Nature **526**, 682 (2015).
[39] E. K. Irish, J. Gea-Banacloche, I. Martin, and K. C. Schwab, Phys. Rev. B **72**, 195410 (2005).
[40] S. Agarwal, S. M. Hashemi Rafsanjani, and J. H. Eberly, Phys. Rev. A **85**, 043815 (2012).
[41] W. K. Wootters, Phys. Rev. Lett. **80**, 2245 (1998).
[42] A. Mezzacapo, U. Las Heras, J. S. Pedernales, L. DiCarlo, E. Solano, and L. Lamata, Sci. Rep. **4**, 7482 (2014).
[43] D. Greenberger, M. Horne, A. Shimony, and A. Zeilinger, Am. J. Phys. **58**, 1131 (1990).
[44] S. Felicetti, M. Sanz, L. Lamata, G. Romero, G. Johansson, P. Delsing, and E. Solano, Phys. Rev. Lett. **113**, 093602 (2014).
[45] D. Z. Rossatto, S. Felicetti, H. Eneriz, E. Rico, M. Sanz, and E. Solano, arXiv:1511.03825 (2015).
[46] J. Kempe, Phys. Rev. A **60**, 910 (1999).
[47] S. Y. Hao, Y. Xia, J. Song, and N. B. An, J. Opt. Soc. Am. B **30**, 2 (2013).
[48] L. Pedersen and C. Rangan, Quantum Info. Process. **7**, 33 (2008).
[49] T. Monz, K. Kim, W. Hansel, M. Riebe, A. S. Villar, P. Schindler, M. Chwalla, M. Hennrich, and R. Blatt, Phys. Rev. Lett. **102**, 040501 (2009).
[50] A. Joshi and M. Xiao, Phys. Rev. A **74**, 052318 (2006).
[51] S. S. Ivanov, P. A. Ivanov, and N. V. Vitanov, Phys. Rev. A **91**, 032311 (2015).
[52] M. Dukalski, and Y. M. Blanter, arXiv:1301.4857 (2013).
[53] Z. Deng, Opt. Comm. **54**, 222 (1985).
[54] Q. H. Chen, Y. Yang, T. Liu, and K. L. Wang, Phys. Rev. A **82**, 052306 (2010).
[55] C. H. Bennett, G. Brassard, C. Crepeau, R. Jozsa, A. Peres, and W. K. Wootters, Phys. Rev. Lett. **70**, 1895 (1993).
[56] M. A. Nielsen and I. L. Chuang, *Quantum Computation and Quantum Information* (Cambridge University Press, Cambridge, 2000).
[57] R. Horodecki, P. Horodecki, M. Horodecki, and K. Horodecki, Rev. Mod. Phys. **81**, 865 (2009).
[58] P. Rungta, V. Bužek, C. M. Caves, M. Hillery, and G. J. Milburn, Phys. Rev. A **64**, 042315 (2001).
[59] T. J. Osborne, Phys. Rev. A **72**, 022309 (2005).
[60] G. Liberti, R. L. Zaffino, F. Piperno, and F. Plastina, Phys. Rev. A **76**, 042332 (2007).